

# The $^{19}\text{F}(\alpha, p_1\gamma)^{22}\text{Ne}$ reaction and the abundance of fluorine in Asymptotic Giant Branch (AGB) stars.

C. Ugalde, A. Couture, J. Görres, E. Stech, and M. Wiescher  
*Department of Physics, University of Notre Dame,  
 Notre Dame, IN 46556, USA*

Recibido el 31 de enero de 2005; aceptado el 3 de abril de 2005

The  $^{19}\text{F}(\alpha, p_1\gamma)$  reaction was investigated in the energy range  $E_\alpha = 1.15 - 2.00$  MeV. Eight resonances were found in the gamma excitation curve, five of which were not observed before. Energy and strength of the resonances were obtained and compared well to values available elsewhere (Kuperus, J., *Physica 31*, (1965) 1603).

*Keywords:* Asymptotic Giant Branch; Nuclear Astrophysics; Fluorine.

La reacción  $^{19}\text{F}(\alpha, p_1\gamma)$  ha sido investigada en el intervalo de energía  $E_\alpha = 1.15 - 2.00$  MeV. Se observaron ocho resonancias en la función de excitación, de las que cinco eran desconocidas a la fecha. Las energías e intensidades de las resonancias fueron obtenidas y son comparables con otros valores medidos previamente (Kuperus, J., *Physica 31*, (1965) 1603).

*Descriptores:* Astrofísica nuclear, Fluor.

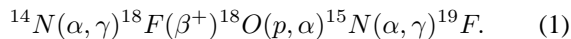
PACS: 26.50.+x; 27.20.+n

## 1. Introduction

The only stable isotope of fluorine,  $^{19}\text{F}$ , is by far the least abundant of stable nuclides in the 12-32 atomic-mass range. Fluorine is fragile and can be destroyed easily by capturing protons at regular stellar temperatures. Useful atomic lines of fluorine are nonexistent in the visible region of the spectrum, and as a result, information on the abundance of fluorine is scarce. Nevertheless, available data [2] provide strong evidence that fluorine is produced deeply within the interiors of AGB stars during helium flashes.

It has been also proposed that  $^{19}\text{F}$  could be produced by nucleon emission from  $^{20}\text{Ne}$  during a type II supernova (SNII) explosion [3]. If this were the case the abundance of fluorine and other elements produced in SNII (like oxygen) would be correlated. However, this is not the case. This suggests that fluorine was synthesized in a site different from a SNII [2].

Thermal pulses of the helium-burning shell in low-mass AGB stars have been proposed [2] as an alternate scenario for  $^{19}\text{F}$  production through the chain



Protons are produced through the reaction



and the required neutrons come from



$^{19}\text{F}$  could be easily destroyed in stars by proton or alpha capture on



and



In a helium-rich environment where protons have been depleted by hydrogen burning and  $^{18}\text{O}$ , the  $^{19}\text{F}(p, \alpha)$  reaction is not likely to occur. The ratio of reaction rates for  $^{15}\text{N} + \alpha$  to  $^{19}\text{F} + \alpha$  sets an upper limit on the temperature at which these reactions take place. The first reaction has been measured while the second remains unknown at the energies of interest; the temperature is important as further nucleosynthetic processes (such as the s-process) in the region could be better understood.

The abundance of  $^{19}\text{F}$  observed imposes a limit in the lifetime of fluorine against destruction by alpha capture as long as the convection mechanism that drives  $^{19}\text{F}$  to the surface of the star and allows us to observe fluorine, is correctly understood. This means that the higher the abundance of fluorine we observe, the lower is the destruction rate of  $^{19}\text{F}$  by alpha capture. For this reason, the rate of the  $^{19}\text{F}(\alpha, p)^{22}\text{Ne}$  reaction is required. At present this reaction rate is still unknown for energies that correspond to a helium-flash environment.

Depletion of  $^{19}\text{F}$  by alpha capture occurs through resonant states of  $^{23}\text{Na}$  in a region of high density of states. These resonant states can proceed to the ground ( $p_0$  protons) and first excited state ( $p_1$  protons) of  $^{22}\text{Ne}$ . Possible scenarios for studying the  $^{19}\text{F}(\alpha, p)^{22}\text{Ne}$  reaction include the detection of both  $p_0$  and  $p_1$  protons. However, the approach followed in this work consisted of the measurement of the  $p_1$  channel by the detection of the  $\gamma$  transition from the first to the ground state in  $^{22}\text{Ne}$  ( $^{19}\text{F}(\alpha, p_1\gamma)^{22}\text{Ne}$ ).

Up-to-date available data for the reaction  $^{19}\text{F}(\alpha, p)^{22}\text{Ne}$  include alpha energies down to 1.3 MeV in the laboratory reference system [1]. However, the alpha energy at which the reaction  $^{19}\text{F}(\alpha, p)^{22}\text{Ne}$  takes place (Gamow window) in a

helium flash ranges from 320 to 760 keV. For this reason the reaction needs to be studied at lower energies.

## 2. Experimental details

The experiment consisted of three parts. The first included the measurement of the reaction yield from 2009 keV to 1238 keV of alpha energy with a Ge detector. In the second stage a BGO scintillator was used to measure the reaction yield from 1700 keV to 1648 keV and from 1354 keV to 1150 keV of beam energy. Larger detection efficiency for the low yield at these energies made up for the loss in energy resolution. The last stage included gamma detection with a Ge detector and was used to scan several times through the resonances found in previous stages of the experiment. This allowed us to study the thickness and stability of the target. On the other hand, the 2 - 4  $\mu\text{A}$  alpha beam was produced by the 4 MV KN Van de Graaff accelerator at the University of Notre Dame.

Two targets with a thickness of 25 keV each were prepared simultaneously by evaporating calcium fluoride onto tantalum sheets. One target was used for the first and second parts of the experiment while the other remained wrapped in aluminum foil and then used in the last stage of the experiment. Tantalum was selected as a substrate for evaporating the thin target layer for its high melting temperature and, therefore, its stability at high beam currents. A 150  $\text{cm}^3$  brass cylindrical scattering chamber was used for the experiment. The far end of the cylinder was tilted  $45^\circ$  from the beam direction and served both as a target holder and faraday cup. The scattering chamber and the detector were shielded with lead bricks to prevent environment radiation from being registered. A liquid nitrogen trap was placed at the end of the beam line close to the scattering chamber and protected the target from carbon build up.

## 3. Reaction yield

The experimental yield  $Y$  for gammas was obtained with

$$Y = \frac{N_y(\theta)}{N_p \epsilon_y}, \quad (6)$$

where  $N_y(\theta)$  is the number of events registered in the detector,  $N_p$  is the number of impinging alphas, and  $\epsilon_y$  is the efficiency of the detector.

The efficiency  $\epsilon_y$  was measured by placing a  $^{60}\text{Co}$  source of known activity at the target position. A spectrum was taken and values of  $\epsilon_y$  were obtained for  $E_\gamma = 1173$  keV and 1332 keV.

The efficiency calibration with the  $^{60}\text{Co}$  source was corrected for summing effects. Let  $A_1$  and  $A_2$  be the count rates measured for the peaks at 1173 keV and 1332 keV, respectively,  $N_0$  the activity of the radioactive source, and  $\epsilon_1$  and  $\epsilon_2$  the corrected efficiencies at both energies, respectively. If the probability of detecting a gamma from the source anywhere

in the spectrum is given by  $\epsilon_T$  then

$$A_1 = N_0 \epsilon_1 - N_0 \epsilon_1 \epsilon_T \quad (7)$$

$$A_2 = N_0 \epsilon_2 - N_0 \epsilon_2 \epsilon_T \quad (8)$$

$$A_3 = N_0 \epsilon_1 \epsilon_2 \quad (9)$$

such that  $A_3$  is the count rate for the summing peak [5]. The efficiencies obtained are  $1.10 \times 10^{-2}$  and  $1.01 \times 10^{-2}$  at 1173 and 1332 keV, respectively.

Detector efficiencies were corrected for angular correlation effects [6], [7] as well. Let  $w(\theta)$  be the probability per unit solid angle that two successive gammas are emitted from the source at an angle  $\theta$ .

An expansion of  $w(\theta)$  is given by

$$w(\theta) = 1 + \frac{1}{8} \cos^2(\theta) + \frac{1}{24} \cos^4(\theta) \quad (10)$$

but as the detector has a finite size, then let us define the correction factor  $W$  by

$$W = \frac{\int_0^R 2\pi r w(\theta) dr}{\int_0^R 2\pi r dr}, \quad (11)$$

where  $R$  is the radius of the detector crystal. The activity  $N_0$  of the source in equations 7-9 was replaced by  $WN_0$  with  $W = 1.09$ . The efficiencies corrected for angular correlation effects are  $1.06 \times 10^{-2}$  and  $9.7 \times 10^{-3}$  at 1173 and 1332 keV, respectively.

The radioactive source proved to be ideal for the calibration of the gamma produced by the  $^{19}\text{F}(\alpha, p_1\gamma)$  reaction has an energy that falls between the  $^{60}\text{Co}$  lines.

At these gamma energies the relation

$$\log \epsilon = a(\log E) + b \quad (12)$$

holds for the Ge detector used [8]. Here  $\epsilon$  is the detection efficiency,  $E$  is the energy of the gamma, and  $a$  and  $b$  are constants. Therefore, the efficiency at 1274 keV can be interpolated to give  $9.98 \times 10^{-3}$ . The experimental data points below  $E_\alpha = 1.33$  MeV were obtained with a BGO detector at the same position of the Ge detector used in previous runs. The yield curve from the BGO was renormalized to match the germanium detector's curve.

The final yield curve is shown in Fig. 1.

## 4. Resonances and strengths

Eight resonances can be identified for the gamma yield from the  $^{19}\text{F}(\alpha, p_1\gamma)^{22}\text{Ne}$  reaction in the range  $E_\alpha = 1200 - 1900$  keV. To obtain the resonance strengths from the yield curve we need to consider that the target thickness may affect the yield value. Corrections for target thickness are required as well.

Let  $Y$  be the thin-target yield (where the energy loss in the target is much smaller than the resonance width) such that

$$Y = \sigma \frac{dE}{\epsilon} \quad (13)$$

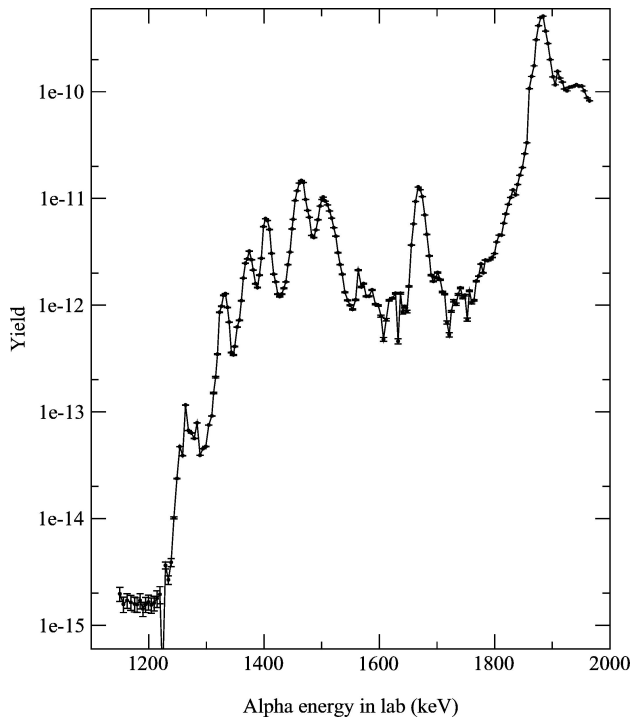


FIGURE 1. Gamma-yield curve from  $^{19}\text{F}(\alpha, p_1\gamma)^{22}\text{Ne}$  between 1.1 MeV and 2.0 MeV of beam energy.

where  $dE$  is the projectile energy loss in the target,  $\epsilon$  is the stopping cross section, and  $\sigma$  is the reaction cross section.

To describe the yield for a thick target (where the thin-target condition stated above is not fulfilled) the thin-target yield has to be integrated over the target thickness  $\Delta$ :

$$Y(E_0) = \int_{E_0-\Delta}^{E_0} \frac{\sigma(E)}{\epsilon(E)} dE. \quad (14)$$

Using the Breit-Wigner formula for  $\sigma(E)$  and assuming  $\epsilon(E)$  to be constant in the resonance region we get

$$Y(E_0) = \frac{\lambda^2}{2\pi} \omega\gamma \frac{M+m}{M} \frac{1}{\epsilon} \times \left[ \arctan \frac{E_0 - E_R}{\Gamma/2} - \arctan \frac{E_0 - E_R - \Delta}{\Gamma/2} \right]. \quad (15)$$

Here  $E_0$  is the energy of the projectile,  $\Gamma$  is the natural width of the resonance,  $E_R$  is the energy of the resonance,  $\omega\gamma$  is the strength of the resonance,  $M$  is the mass of the target,  $m$  is the mass of the projectile, and  $\lambda$  is the Compton wavelength of the projectile.  $E_R$ ,  $\Gamma$ ,  $\omega\gamma$ , and  $\Delta$  were treated as parameters and the yield curve was fitted to the yield expression above. The strengths and resonance energies are shown in Table I. Data from [1] are shown in Table II.

TABLE I. Resonance energy versus strength from this work.

Resonance Energy (keV)	Strength from this work (eV) $\pm 20\%$
1270	0.04
1330	0.2
1372	0.3
1401	0.3
1462	2.1
1503	1.4
1668	2.7
1880	60

TABLE II. Resonance Energy versus strength from [1].

Resonance Energy (keV)	Strength from [1] (eV) $\pm 40\%$
1492	1.3
1507	0.26
1574	$< 0.7$
1879	$< 4$
1884	27

## 5. Conclusions

We found eight resonances for the  $^{19}\text{F}(\alpha, p_1\gamma)^{22}\text{Ne}$  reaction for a beam energy between 1200 and 1900 keV, five of which, at 1270, 1330, 1372, 1401, 1462 and 1668 keV, had not been observed before. The resonance strengths were obtained.

Interference between neighbor resonances could affect the obtained strengths. An R-Matrix analysis of the yield curve should help to reduce the uncertainties in our results. Future plans include the study of the  $^{19}\text{F}(\alpha, p_1)^{22}\text{Ne}$  and  $^{19}\text{F}(\alpha, p_0)^{22}\text{Ne}$  reactions in the same beam-energy region and lower energies. Protons from the reaction could be detected with several silicon barrier detectors at various angles, so both strengths of the resonances and angular distributions can be measured. We expect elastically scattered alphas to reach the detectors with a higher rate than protons; nickel or gold foils in front of the detectors could be useful as shielding.

As calcium fluoride targets showed to be unstable when they were left exposed to environment humidity, other experiments should be carried with freshly-made targets or with targets being kept under vacuum or argon while not being irradiated with beam.

1. J. Kuperus, *Physica* **31** (1965) 1603.
2. A. Jorissen *et al.*, *Astron. Astrophys.* **261** (1992) 164.
3. S.E. Woosley *et al.*, *Astrophys. J.* **356** (1990) 272.
4. G.J. Mathews, *Nature* **359** (1992) 18.
5. G. Gilmore, and J. Hemingway, *Practical gamma-ray spectrometry*, John Wiley and Sons Ltd (1995).
6. E.L. Brady, and M. Deutsch, *Phys. Rev.* **78** (1950) 558.
7. C.N. Yang, *Phys. Rev.* **74** (1948) 764.
8. EG&G Ortec Catalog, *Modular Pulse-Processing Electronics and Semiconductor Radiation Detectors* (1995).
9. C.E. Rolfs, and W.S. Rodney, *Cauldrons in the Cosmos*, University of Chicago Press(1988).